

X-ray variability of Capella[★]

A. J. J. Raassen^{1,2} and J. S. Kaastra¹

¹ SRON Netherlands Institute for Space Research, Sorbonnelaan 2, 3584 CA Utrecht, The Netherlands
e-mail: a.j.j.raassen@sron.nl

² Astronomical Institute Anton Pannekoek, Kruislaan 403, 1098 SJ Amsterdam, The Netherlands

Received 23 May 2006 / Accepted 21 September 2006

ABSTRACT

We discuss 12 individual observations of stable calibration source Capella over the last five years. The light curves and spectra, derived from *LETGS* on board *CHANDRA* are investigated. The spectra cover the wavelength range 1–175 Å. Nine of the twelve observations show comparable count rates, while the three most recent observations between March 2005 and April 2006 show a 40–50% higher count rate. No individual flares were recognised. Line flux ratios between different observations show that the variations are related to the hotter plasma. Variations in line fluxes of highly ionised iron lines show a strong resemblance with earlier line flux variations in the years 1992–1995. A time interval of 10.7(2) year is determined between two maxima in line fluxes. Emission measure modellings to the total spectra have been made by means of *SPEX* in combination with *MEKAL*. Observations with higher count rates have a higher emission measure at higher temperature.

Key words. stars: individual: Capella – stars: coronae

1. Introduction

The first line rich X-ray source observed by *CHANDRA* and *XMM-Newton* was Capella, a G1III+G8III giant binary system. The spectrum of this source shows an overwhelming amount of emission lines in the range from 0.07 to 12 keV, i.e. from 1 to 175 Å. Therefore Capella serves as source for calibrating and testing (resolving power, response matrix, line spread function, etc) the instruments aboard the new X-ray space observatories (Canizares et al. 2005). It is described in the first light papers on high resolution (grating) spectroscopy of both satellites (Canizares et al. 2000 (HETG); Brinkman et al. 2000 (LETG) and Audard et al. 2001 (RGS)). Thanks to the many resolved line features, the spectra offer the possibility to investigate the coronal plasma into detail. These investigations have resulted in a number of papers on temperatures, emission measures and abundance determinations of the corona of Capella, based on X-ray spectra from *CHANDRA* and *XMM-Newton* (e.g. Behar et al. 2001; Mewe et al. 2001; Ness et al. 2001; Desai et al. 2005). Over these years Capella has shown to be stable without any evidence of flaring. However, in the past some variation (Linsky et al. 1998; Johnson et al. 2002; Brickhouse et al. 2000) was noticed, but also without flaring.

Before the *CHANDRA* and *XMM-Newton* era Linsky et al. (1998) have investigated the Capella spectrum with *EUVE* over the years 1992 to 1995. They focussed on the fluxes of a number of Fe lines at 128.73, 97.88, 102.22, 142.27, 108.37, 93.92 Å and determined the emission measures from these Fe line fluxes at different times. Based on the variability of the volume emission measures, they conclude to variability in the coronal emission measure at the hotter temperatures.

Linsky et al. (1998) and Johnson et al. (2002) investigated the Fe XXI line at 1354 Å using the Hubble Space

Telescope/Space Telescope Imaging Spectrograph in 1995 and 1999, respectively. Comparing both observations Johnson et al. (2002) notice a decline by a fairly large factor of the emission of this line related to the G8III star in the binary system. Ishibashi et al. (2006) assume that the G8III star is the strongest X-ray source, but that the G1III star significantly contributes to the hotter emission at $T \gtrsim 10^7$ K.

In this paper we investigate the high resolution X-ray spectra of Capella observed by *LETGS* on board *CHANDRA* over the last six years. We include in this paper the investigations of light curves, the investigations of individual line fluxes and line flux ratios, as well as overall spectral fittings to the total spectra by means of *SPEX*.

In Sect. 2 the observations are discussed and the log of the observations is given. In Sect. 3 we describe the light curves and their fluctuations. Section 4 shows the individual line fluxes and their behaviour over the years, while in Sect. 5 a DEM-modelling to the total spectra is discussed.

2. Observations

Twenty one spectra of Capella were obtained with *LETG* on board *CHANDRA* over a period of several years, from the launch of *CHANDRA* in 1999 till now, as part of the calibration program. Here we focus on the twelve LETG-spectra that were detected with *HRC-S* and that have exposure times $\gtrsim 20$ ks.

We used the archival data (including the CIAO pipelining) over the years 1999–2006. Light curves and spectra were extracted for all (twelve) observations of this calibration source. The log of the observations is shown in Table 1. Eleven of the observations have durations between 25 and 35 ks, and one long observation in November 1999 (Obs ID=1248) has a duration of 85 ks. Seven observations are on-axis, while five are off-axis. The offset in Table 1 is given in arcmin. A minus sign indicates a lower chip coordinate and a lowering of the upper wavelength

[★] Table 1 and Fig. 2 are only available in electronic form at <http://www.aanda.org>

Table 3. Line fluxes of Obs ID=1248 and 5956 in units of 10^{-13} ergs cm^{-2} s^{-1} as measured at Earth. The last column gives the line flux ratios, as used in Fig. 4. The values within brackets are the 1σ errors.

ion	λ	T_{opt}	flux 1248	flux 5956	ratio
Fe IX	171.075	5.86	3.56(.42)	4.07(.72)	1.13(.24)
C VI	33.736	6.13	4.78(.26)	5.82(.52)	1.19(.12)
N VI	28.787	6.17	1.18(.14)	1.07(.26)	0.90(.24)
N VI	29.520	6.17	1.06(.14)	1.16(.28)	1.10(.31)
N VII	24.781	6.32	5.23(.27)	6.37(.52)	1.22(.12)
O VII	21.602	6.33	8.16(.35)	8.13(.62)	1.00(.09)
O VII	22.101	6.33	5.62(.30)	6.31(.55)	1.12(.11)
Fe XVI	50.350	6.45	2.28(.14)	2.59(.26)	1.14(.13)
Fe XVI	50.555	6.45	0.83(.11)	1.05(.20)	1.28(.30)
Fe XVI	66.263	6.46	1.30(.14)	1.37(.34)	1.05(.28)
Fe XVI	66.368	6.46	1.84(.16)	2.14(.38)	1.16(.23)
O VIII	18.969	6.48	27.18(.53)	31.94(1.0)	1.18(.04)
Fe XVII	15.013	6.72	47.40(1.0)	55.22(1.5)	1.16(.04)
Fe XVII	16.775	6.72	26.80(.55)	33.23(1.8)	1.24(.05)
Fe XVII	17.051	6.72	37.31(1.1)	44.97(2.8)	1.21(.08)
Fe XVII	17.101	6.72	30.91(1.1)	38.98(2.7)	1.26(.10)
Ne X	12.134	6.77	18.73(.58)	22.55(1.2)	1.20(.07)
Fe XVIII	93.923	6.80	8.50(.23)	10.64(.44)	1.25(.06)
Fe XVIII	103.937	6.80	3.11(.15)	3.62(.30)	1.16(.11)
Fe XIX	108.37	6.89	5.51(.20)	7.10(.38)	1.29(.08)
Fe XX	118.66	6.95	1.08(.11)	1.80(.29)	1.67(.32)
Fe XX	121.83	6.95	2.20(.16)	3.46(.31)	1.57(.18)
Mg XII	8.421	7.01	5.01(.33)	7.80(.75)	1.55(.18)
Fe XXI	128.73	7.02	2.19(.18)	4.13(.42)	1.89(.24)
Fe XXII	117.17	7.08	1.33(.13)	2.54(.24)	1.91(.26)
Si XIV	6.182	7.21	1.87(.24)	3.73(.56)	2.00(.40)

a limited wavelength range. A power law distribution was added to adjust for the continuum.

The obtained fluxes were used to calculate the line flux ratios between the lines of observations Obs ID=1248, the on-axis observation with the longest exposure time, and Obs ID=5956. The latter being one of the three observations with higher zeroth order count rate, but just like Obs ID=1248 on-axis. For the off-axis observations telescope vignetting might influence the fluxes of the Si XIV and Mg XII lines at 6.182 and 8.421 Å, respectively. There may also be a small uncertainty of the cross-dispersion factor for off-axis observations. The line fluxes are collected in Table 3 in order of increasing optimal line formation temperature (T_{opt}), given on a log scale. This is the temperature of the peak of the emissivity distribution. The underlying calculations of the ionisation balance are from Arnaud & Rothenflug (1985) and Arnaud & Raymond (1992). The line flux ratios versus the optimal line formation temperature are plotted in Fig. 4. The errors on the temperature are arbitrarily chosen to be 0.1 dex.

The figure shows that the line flux ratios are constant for values of $\log T$ below 6.8. In this temperature domain the line fluxes of observation Obs ID=5956 are a factor of 1.16(.09) higher than for observation Obs ID=1248. Above $\log T = 6.8$ the line flux ratio 5956/1248 increases to about a factor of 2. This indicates that no overall increase of the emission measure (by a constant factor) is present, but that the increase of the emission measure depends on the temperature. It is higher for the hottest temperature component.

This is in agreement with the conclusions of Linsky et al. (1998) and Johnson et al. (2002). They investigated the Fe XXI line at 1354 Å observed by *HST*. Thanks to the more

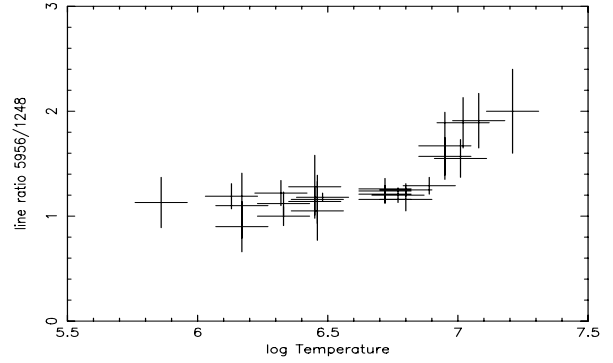


Fig. 4. The line flux ratio between observation Obs ID=5956 and Obs ID=1248 versus the optimal formation temperature.

dispersive wavelength range of the Fe XXI line at 1354 Å Johnson et al. (2002) could assign the variability in emission to the G8III component of the binary system, the star with the hotter coronal plasma. Their conclusion was based on a comparison of their data with those from the earlier observations by Linsky et al. (1998). Ishibashi et al. (2006) assume that the G8III star is the strongest X-ray source, but that the G1III star significantly contributes to the hotter emission at $T \gtrsim 10^7$ K.

4.2. Line fluxes versus time

Apart from a comparison of the line flux ratios of a large number of lines of the observations Obs ID=1248 and Obs ID=5956 versus the temperature (this work) we have measured for all twelve *LETGS* observations the fluxes of the lines at 93.92 Å (Fe XVIII), 108.37 Å (Fe XIX), and 128.73 Å (Fe XXI). They were observed by Linsky et al. (1998) and Brickhouse et al. (2000) and were indicated to be unblended. The results of the series using *EUVE* (Linsky et al. 1998; Brickhouse et al. 2000) and of this work are collected in Table 4. The fluxes are given in units of 10^{-13} erg cm^{-2} s^{-1} .

Although calibration differences between *EUVE* and *LETGS* can not be ruled out, the fluxes obtained by *EUVE* (Linsky et al. 1998; Brickhouse et al. 2000) are close to the values given in this paper and they are variable over time. According to our conclusions from Fig. 4 the fluxes of the Fe XXI line at 128.73 Å are most sensitive for variations, due to the high formation temperature. This way we may study the behaviour of the line fluxes versus the time. The behaviour of the flux of the line at 128.73 Å versus the time is given in Fig. 5. This figure covers a range of about 15 years. However, there are also severe gaps in observations between March 1996 and September 1999 and between March 1994 and December 1995. Figure 5 shows two clear peaks. To determine the peak values the peaks were fitted with a Gaussian. Due to the absence of *EUVE* observations between March 1994 and December 1995 (the time of maximum) the peak profiles are forced to have the same shape, by coupling the peak value and the half-width at half maximum. The date of our peak, determined this way, is 16 September 2005 (19 days), while the half-width at half maximum is 215 (19) days. The time difference between the two peaks is 10.7(.2) years. These results are in good agreement with predictions by Raassen & Kaastra (2006), made before the observation in April 2006.

Table 4. Line fluxes for the Fe XXI line at 128.73 Å, the Fe XIX line at 108.37 Å, and the Fe XVIII line at 93.92 Å in Capella. The fluxes indicated by *EUVE* are from Linsky et al. (1998) and from Brickhouse et al. (2000), while the others are from this work. The fluxes are corrected for interstellar absorption ($N_{\text{H}} = 1.8 \times 10^{18} \text{ cm}^{-2}$).

Obs ID	Date	flux ^a		
		128.73 Å	108.37 Å	93.92 Å
EUVE ^b	1992-12-11	2.2(0.3)	4.4(0.3)	7.3(0.4)
EUVE ^b	1993-12-23	2.5(0.3)	3.5(0.3)	5.3(0.4)
EUVE ^b	1994-02-15	4.8(0.5)	6.1(0.4)	8.4(0.6)
EUVE ^b	1994-02-26	4.6(0.4)	6.8(0.4)	8.4(0.6)
EUVE ^b	1995-12-02	3.7(0.4)	7.8(0.4)	10.1(0.6)
EUVE ^c	1996-03-05	2.6(0.2)	5.5(0.2)	10.2(0.3)
62435	1999-09-06	2.1(0.3)	5.5(0.3)	8.5(0.4)
1420	1999-10-30	2.6(0.4)	5.4(0.3)	9.2(0.4)
1248	1999-11-10	2.4(0.2)	5.9(0.2)	8.9(0.2)
0058	2000-03-08	2.4(0.3)	5.4(0.3)	8.2(0.4)
1009	2001-02-14	2.1(0.3)	4.6(0.3)	8.4(0.4)
2582	2002-10-05	2.0(0.4)	5.6(0.4)	9.1(0.4)
3479	2002-10-06	2.2(0.5)	5.2(0.4)	8.6(0.5)
3675	2003-09-28	1.7(0.3)	4.7(0.3)	7.9(0.4)
5041	2004-09-11	3.0(0.4)	6.6(0.4)	9.3(0.4)
5956	2005-03-31	4.6(0.4)	7.6(0.4)	11.1(0.4)
6165	2005-10-02	5.4(0.5)	9.2(0.4)	12.5(0.5)
6472	2006-04-24	4.2(0.4)	7.7(0.4)	10.5(0.4)

^a In units of $10^{-13} \text{ erg cm}^{-2} \text{ s}^{-1}$.

^b From Linsky et al. (1998).

^c From Brickhouse et al. (2000).

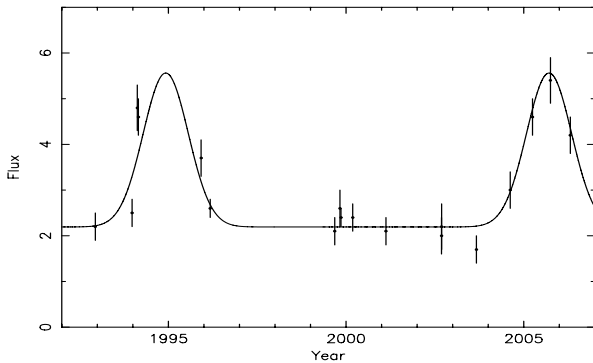


Fig. 5. The line flux of Fe XXI line $\lambda = 128.73$ versus time. Over the years 1992 to 1995 we use the data from *EUVE* (Linsky et al. 1998), for one data point in 1996 from *EUVE* (Brickhouse et al. 2000) and over the years 1999 to 2005 we use the data from *LETGS* aboard *CHANDRA* (this work). The fluxes are in units of $10^{-13} \text{ erg cm}^{-2} \text{ s}^{-1}$.

5. DEM-modelling

To have some other confirmation for our conclusion that the increase in emission is related to the hotter plasma (see Fig. 4) we analyze the total *LETGS* spectra of Obs ID=1248 and Obs ID=6165 by means of a differential emission measure (DEM) modelling, using SPEX (Kaastra et al. 1996a) in combination with MEKAL (Mewe et al. 1985, 1995; Kaastra et al. 1996b). MEKAL calculates a continuum and models more than 5400 spectral lines, and is available on the WWW². The applied model is a Collisional Ionisation Equilibrium (CIE) model for optically thin plasma. The ionisation equilibrium is based on calculations by Arnaud & Rothenflug (1985) and Arnaud & Raymond (1992). In an earlier investigation of the temperature structure of the corona of Capella (Audard et al. 2001) a three

² <http://www.sron.nl/divisions/hea/spex/>

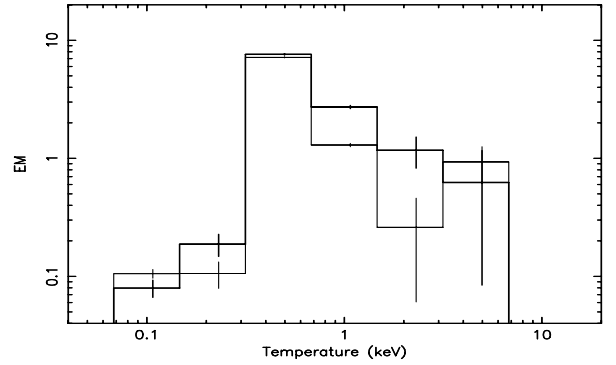


Fig. 6. DEM modelling to two spectra of Capella. The thin line corresponds to Obs ID=1248 and the bold line to Obs ID=6165. *EM* is given in units of 10^{52} cm^{-3} .

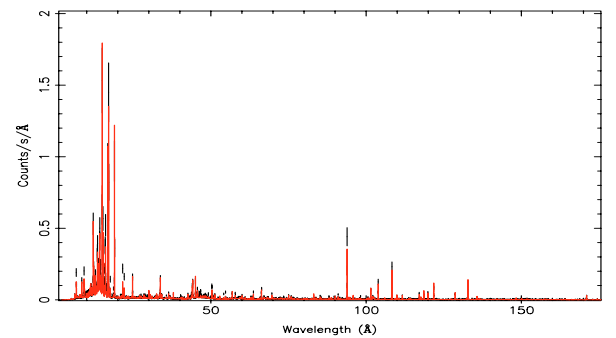


Fig. 7. Modelled and observed spectrum of observation Obs ID=1248. The solid line (red in the electronic version) is the model.

temperature model was applied to RGS spectra obtained March 2000, close to the dates of our observations Obs ID=1248 and Obs ID=0058.

For our differential emission measure (DEM) modelling we use the module “regularisation” (e.g., Kaastra et al. 1996b) in SPEX. This module uses a matrix inversion with an additional constraint that the second derivative of the solution is as smooth as possible. The emission measure is defined as $EM = n_e n_H V$ in which $n_H = 0.85 \times n_e$. The model spectrum (including the 5400 lines of MEKAL) is fitted to the total spectrum, line features and continuum, minimising the χ^2 value. A wavelength correction (a multiplication factor of -4.6×10^{-4} for Obs ID=1248 and of -1.05×10^{-3} for Obs ID=6165) was added to correct for wavelength deviations. Abundances by Audard et al. (2001) based on *XMM-Newton* and by Argiroffi et al. based on *LETGS* agree except for the value of Si. It is clear from Fig. 1 in Audard et al. (2001) that the value of Argiroffi et al. (2003) is better. We applied these abundances for the DEM-modelling.

The result for the *EM* (per logarithmic temperature bin) is shown in Fig. 6. The *EM* is given in units of 10^{52} cm^{-3} . The bold line is related to the DEM of the spectrum of observation Obs ID=6165. The thinner line belongs to observation Obs ID=1248. The summed *EM* of the observation Obs ID=1248 is $9.8(0.4) \times 10^{52} \text{ cm}^{-3}$, close to the value $9.60(0.13) \times 10^{52} \text{ cm}^{-3}$ determined by Audard et al. (2001) and the $10.8(0.7) \times 10^{52} \text{ cm}^{-3}$ by Argiroffi et al. (2003). From this figure it is clear that the observation of Obs ID=6165 has a significantly higher emission than observation Obs ID=1248 around 1 keV.

Figure 7 shows the observed and modelled spectrum of observation Obs ID=1248, based on the DEM-modelling.

Table 5. Calculated and measured line fluxes of Obs ID=1248 and 6165 in units of 10^{-13} erg cm $^{-2}$ s $^{-1}$.

ion	λ	flux 1248		flux 6165		ratio	
		calc.	meas.	calc.	meas.	calc.	meas.
Fe IX	171.075	4.4	3.6	2.5	2.3	0.6	0.6
C VI	33.736	5.2	4.8	5.3	4.7	1.0	1.0
N VII	24.781	5.1	5.2	6.3	5.3	1.2	1.0
O VII	21.602	4.6	8.2	3.9	8.7	0.9	1.1
O VIII	18.969	34.9	27.2	38.0	31.2	1.1	1.1
Fe XVII	15.013	58.4	47.4	64.1	51.8	1.1	1.1
Fe XVII	16.775	29.8	26.8	32.2	30.6	1.1	1.1
Ne X	12.134	22.0	18.7	25.3	25.6	1.2	1.4
Fe XVIII	93.923	7.8	8.5	9.0	11.9	1.2	1.4
Fe XIX	108.37	5.6	5.5	7.6	8.6	1.4	1.6
Fe XX	121.83	3.8	2.2	6.3	4.4	1.7	2.0
Mg XII	8.421	4.8	5.0	7.3	6.9	1.5	1.4
Fe XXI	128.73	3.1	2.2	6.6	4.8	2.1	2.2
Fe XXII	117.17	1.4	1.3	3.1	3.4	2.2	2.6
Si XIV	6.182	1.6	1.9	3.1	3.2	1.9	1.7

The calculated and measured fluxes of the observations OBS ID=1248 and 6165 are collected in Table 5. Keeping in mind that the theoretical transition probabilities are often off by 25% the agreement between the calculated and measured fluxes are quite good and reflect the trend given in Fig. 4.

5.1. Conclusions

Twelve spectra of calibration source Capella, observed since 1999 with *LETGS* aboard *CHANDRA*, have been studied. They show clear variations in count rates as well as in fluxes of individual highly ionised Fe lines.

The light curves for all observations are flat (at different count rate level) without the presence of individual flares. However, over years they vary on a scale of 50%. Count rates and line fluxes reached a maximum around 15 September 2005.

The variation in line fluxes depends on the ionisation stages of the ions and the temperature of the peak of the emissivity distribution. The variability is stronger for the hotter coronal plasma.

A model fit through our measured line fluxes of highly ionised Fe lines with measurements by Linsky et al. (1998) and Brickhouse et al. (2000), based on *EUVE* observation, show two peaks with a time interval of 10.7 (.2) year. To conclude whether it concerns an incidental effect or a periodically returning event regular observations till the year 2017 are necessary.

Acknowledgements. The SRON Netherlands Institute for Space Research is supported financially by NWO.

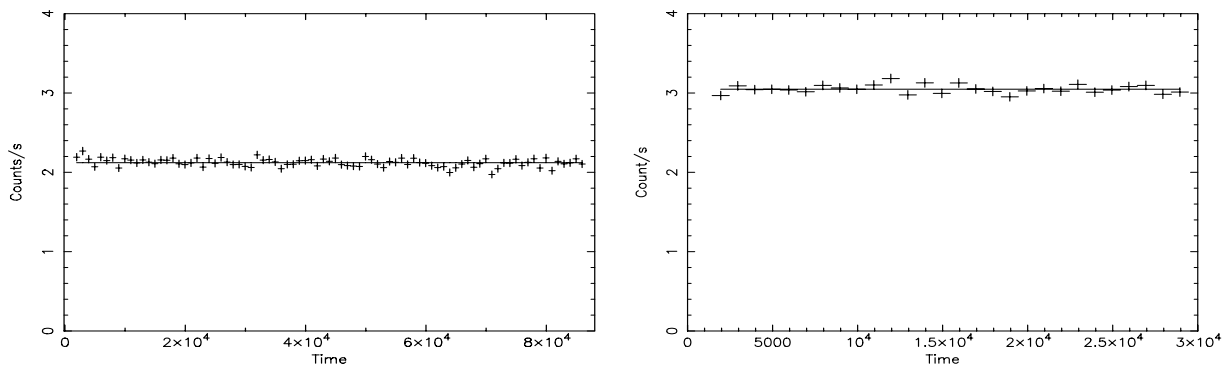
References

- Argiroffi, C., Maggio, A., & Peres, G. 2003, *A&A*, 404, 1049
 Arnaud, M., & Raymond, R. 1985, *ApJ*, 398, 394
 Arnaud, M., & Rothenflug, J. 1992, *A&AS*, 60, 425
 Audard, M., Behar, E., Güdel, et al. 2001, *A&A*, 365, L329
 Behar, E., Cottom, J., & Kahn, S. M. 2001, *ApJ*, 548, 966
 Brickhouse, N. S., Dupree, A. K., Edgar, R. J., et al. 2000, *ApJ*, 530, 387
 Brinkman, A. C., Gunsing, C. J. T., Kaastra, J. S., et al. 2000, *ApJ*, 530, L111
 Canizares, C. R., Davis, J. E., Dewey, D., et al. 2005, *PASP*, 117, 1144
 Canizares, C. R., Huenemoerder, D. P., Davis, D. S., et al. 2000, *ApJ*, 539, L41
 Desai, P., Brickhouse, N. S., Drake, J. J., et al. 2005, *ApJ*, 625, L59
 Ishibashi, K., Dewey, D., Huenemoerder, D. P., & Testa, P. 2006, *ApJ*, 644, L117
 Johnson, O., Drake, J. J., Kashyap, V., et al. 2002, *ApJ*, 565, L97
 Kaastra, J. S., Mewe, R., & Nieuwenhuijzen, H. 1996a, in *UV and X-ray Spectroscopy of Astrophysical and Laboratory Plasmas*, ed. K. Yamashita, & T. Watanabe (Tokyo: Universal Academy Press, Inc.), 411 (SPEX)
 Kaastra, J. S., Mewe, R., Liedahl, D. A., et al. 1996b, *A&A*, 314, 547
 Linsky, J. L., Wood, B. E., Brown, A., & Osten, R. A. 1998, *ApJ*, 492, 767
 Mewe, R., Gronenschild, E. H. B. M., & van den Oord, G. H. J. 1985, *A&AS*, 62, 197
 Mewe, R., Kaastra, J. S., & Liedahl, D. A. 1995, *Legacy*, 6, 16 (MEKAL)
 Mewe, R., Raassen, A. J. J., Drake, J. J., et al. 2001, *A&A*, 368, 888
 Ness, J.-U., Mewe, R., Schmitt, J. H. M. M., et al. 2001, *A&A*, 367, 282
 Raassen, A. J. J., & Kaastra, J. S. 2006, *Workshop on High resolution X-ray spectroscopy: toward XEUS and Con-X*, 27–28 March 2006, MSSL, Dorking, UK

Online Material

Table 1. Dates of observation of Capella by means of *LETGS*.

Obs ID	Date-obs-start	Date-obs-end	Exposure time(ks)	offset ^a
62435	1999-09-06T00:26:00	1999-09-06T09:48:00	32.71	-0.13
1420	1999-10-29T22:30:00	1999-10-30T07:27:00	30.19	-0.04
1248	1999-11-09T13:27:00	1999-11-10T13:28:00	85.23	0.00
0058	2000-03-08T06:29:00	2000-03-08T16:24:00	34.11	-0.08
1009	2001-02-14T11:40:00	2001-02-14T19:26:00	26.97	-0.03
2582	2002-10-04T23:58:00	2002-10-05T08:35:00	28.83	-1.50
3479	2002-10-06T10:03:00	2002-10-06T19:10:00	30.38	1.46
3675	2003-09-28T04:23:00	2003-09-28T12:21:00	27.16	0.05
5041	2004-09-11T06:53:00	2004-09-11T15:15:00	28.88	3.03
5956	2005-03-31T08:09:00	2005-03-31T17:03:00	30.17	0.03
6165	2005-10-02T04:53:00	2005-10-02T12:59:00	29.17	-2.97
6472	2006-04-23T23:30:00	2006-04-24T07:46:00	30.18	1.54

^a given in arcmin.**Fig. 2.** The light curves of Capella of Obs ID=1248 (*left panel*) and of Obs ID=6165 (*right panel*). The time is divided in bins of 1000 s.